Data analysis of ^3He gas-filled detectors

Author: Roger González March
*Facultat de Física, Universitat de Barcelona, Diagonal 645, 08028 Barcelona, Spain.**

Advisor: Ariel Esteban Tarifeño Saldivia and Volodymyr K Magas

Abstract: A Digital Pulse Analysis method has been developed and tested for ^3He gas-filled neutron counters using fast digitizers. The method is needed for the calibration of high pilled-up events in pulsed proton beams. By this procedure identification and reconstruction of events are suit for digital signal processing methods that maintain and add flexibility in front of traditional-analog methods.

I. INTRODUCTION

In this work, it is implemented a methodology for digital pulse analysis in ^3He-filled proportional neutron counters. The methodology is aplied to the construction of the pulse amplitude and charge integrated spectra in neutron counting experiments carried out with radioactive sources at the CERN n_TOF facility.

^3He detectors were one of the most used to detect thermal neutrons via nuclear interactions. In the last years pulse detection via front-end electronics has been replaced by high-performance flash-ADCs (FADC) [1]. n_TOF facility has upgraded its high-performance digital data acquisition system increasing amplitude resolution by 12 bits and sampling rates up to 1 GHz [6]. As a matter of fact, FADCs, have almost negligible dead times and what is even more important, can overcome pulse processing by analog electronics by offline digital pulse processing that increases flexibility to apply any complex method for signal processing such as noise, baseline, and event pile-up.

A. Gas-Filled Neutron Detectors

The issue with neutrons is that they don't interact directly with matter. Therefore, the detection relies on indirect methods.

The gas filled detectors is a great choice for counting thermal neutrons. Gas filled neutron detectors are usually designed in a metal cylindrical shape with two electrodes. The anode is a wire going to the top of the cylinder through the bottom and the cathode is connected to the walls. Between them the cylinder is filled with BF_3 or ^3He that will be responsible of the interaction with the neutrons. The reaction of ^3He with a neutron breaks the nucleus into a tritium and a proton. This reaction is exothermic and release 764 keV that is shared between the tritium and the proton. [2]

$$^3He + n \rightarrow {}^3H + p + 764\,keV \tag{1}$$

The proton and the tritium ionize the gas in their path until they have exhausted all their energy. Choosing the right voltage, we can use ^3He detectors as a proportional counter. In other words, we can create an avalanche ionization that will be linearly proportional to the energy deposited in the gas.

II. EXPERIMENTAL SETUP

The data acquisition for the experiment was carried out in the n-TOF collaboration at the CERN facility under nearly ideal conditions. We have only detected noise corresponding to the portable source needed for the deployment of the setup.

In the experiment, is used three different ^3He proportional counters. LND 252139 (LND), Vacutek 70 V60 (V60), and finally the Vacutek 70 V61 (V61). All of them with neutron moderation to achieve the collection of thermal neutrons. Each of them will have a different pulse amplitude spectrum. One source of 241Am-Be (1 Ci) have been used. The whole setup is composed of a high-performance pulse measurement chain that consists of a Camberra charge preamplifier and two other preamplifiers designed by our team, UPC1 and UPC2 charge type preamplifier.

A. Data Processing

While the experiment is running, DAQ data is stored in magnetic tapes for long-term storage at EOS-CASTOR (CERN open storage technology, 500PB). For each time of acquisition (run) data is split into movies of 200-300 ms. Furthermore, we have a first stage extracting the data from the magnetic tapes and transforming them into raw files consisting mainly of the digitized detector signals. Even more, with help of compression algorithms designed by the n-TOF collaboration and input parameters for our experiment, the data is transformed into readable data files (ROOT files).

*Electronic address: rogeruniub@gmail.com

ROOT files store data hierarchically into a tree form. Typically, our root files will contain 14 trees and each tree will correspond to a movie. Inside this tree, we have different leaves relating to our signal, the baseline, and different information about extraction.

B. Processing time

A standard run of 1h and 30 min will contain an average of 500 root files. With the developed algorithm for the detection of pulses, it usually takes around one hour to loop all movies inside one file and takes 10Gb of RAM. For the calibration 5034 files have been analyzed. That is to say, 210 days of processing time using the standard computing facilities available at CERN (lxplus system).

C. HTCondor

HTCondor is a key service offered by CERN. The Batch Service provides High Throughput Computing to support experiments and users at CERN with a fair-sharing mechanism. It allows users to queue up jobs in the batch farm (around 100k cores). Once a job is submitted is queued until the job is executed into a worker node and returns the output files into the Linux lxplus user directory. Without the service of HTcondor, the analysis of our experiment is not viable. HTCondor has allowed us to submit every root file parallel to each other reducing the processing time, for each run, to less than a day. Only for the calibration, we have used 5034 workers nodes (CPU's) and 50340GB of RAM.

III. METHODS

A. Signal Derivative

The first step of every pulse data analysis is to find some method to differentiate the background and noise from the event electrical waveform. A general approach based on signal differentiation has been successful in other detectors from the facility [4] , therefore the same definition has been used.

$$d_i \equiv \sum_{j=1}^{\min[N,i,P-1-i]} (s_{i+j} - s_{i-j}) \tag{2}$$

Where the derivative of the signal s at the i-th point performs an integration from of length N (step size) at both sides and P is the total number of points of the recorded signal. The curious eye may have noticed that it is not the canonic derivative. Differentiation tends to exaggerate problems with finite sampling and blow up the noise from the signal, therefore smoothing while performing the derivative is required. Nevertheless, the optimal step size must be determined. The election of the step size has been set on the pulse width and manually adjusted until reached optimal signal-to-noise ratio and performance. For an example of implementation, see figure 1.

B. Trigger

While applicating the signal derivate defined in section a blow-up of the signal derivative is expected when a pulse is found. In an effort to discriminate background and noise from pulses a signal derivate threshold is placed.

In a general approach, the election of the threshold can be fixed on the RMS (root mean squared) value from the signal. To find the RMS value of our signal, the derivate values are projected into a histogram. Values that correspond to the noise are expended to a group around 0 in a gaussian distribution and the RMS can be extracted with a fitting. Meanwhile, signal derivative points from our pulses will be distributed outside the Gaussian shape in long tails.

However, due to the nature of our signals, an RMS fitting method is not suitable. Analyzing the projection of the derivative is found that a tail corresponding to the pulses cannot be discriminated from the noise. In fact, only a few events are seen per signal and the smallest pulses are close to the noise values. For these reasons, a manual study is needed. In light of finding the proper value, a threshold value is decided for every different detector model and voltage usage taking into count the signal-noise ratio. Further discussion of the threshold is found in IV A.

C. Moving Average

Our signals are of the slow rise and fall timing therefore it is affected by high-frequency noise. [5]. The moving average is a proper method for smoothing. Furthermore, is one if not the fastest, low pass filter and it is appropriate when dealing with high data points. The definition of the moving average used is:

$$y_i = \frac{1}{2N} \sum_{j=0}^{N-1} (s[i+j] + s[i-j]) \tag{3}$$

Where s is the signal, N (step size) is the number of points used forward and backward in the moving average and y_i is the smoothed signal at the data point i. Like the derivative, the optimal step size is needed. A large

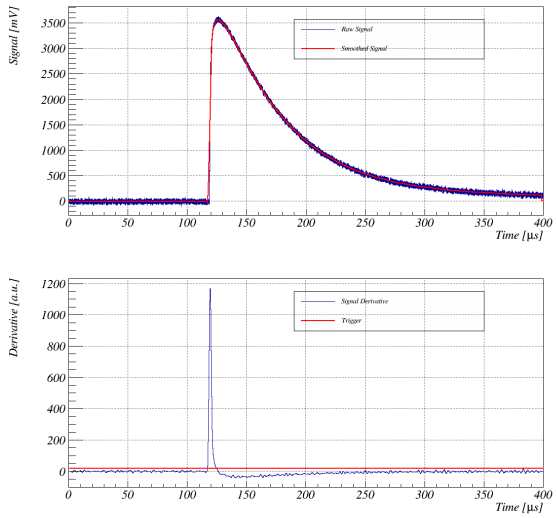

FIG. 1: Top panel, example of a high amplitude pulse from V60 detector. Notice how the rise-time of the signal smoothed is distorted by the Moving Average. Bottom panel derivate of the pulse with the selected Trigger Threshold.

step size could reduce the white random noise to almost negligible, but it also distorts the signal shape making further analysis unworkable. Therefore, the step size selection will be set on a range that is enough to deal with the noise but maintain the shape and reduce the amplitude value to a minimum.
Multiple-pass moving average filter has been tested. That is passing a moving average filter consecutive times in the signal. Multiple-pass filter has better stopband attenuation. However a better smoothing hasn't been observed therefore only one moving average has been applied due to execution speed. For an example of implementation, see figure 1.

D. Baseline amplitude and area

Once an event is detected a smoothing is applied in a window of manually selected presamples and integration time. These parameters are determined in a previous study and will vary from the detector and voltage usage.

To subtract the base line a linear fitting, four points have been set. A first point in the beginning of presamples, the second at the triggering point and the third one after the integration length, and finally at the end of our postsamples (that has the same length than the presamples, for simplicity). After the subtraction of the baseline, we have the pulse prepared to further analysis. In order to obtain the pulse amplitude histogram, the full amplitude of single events is extracted from the analysis. In addition, it is also extracted the total area of single event waveforms, which is proportional to the total charge collected inside the counter resulting from the detection of a radiation event.

There are several ways to extract the amplitude, one could do a parabolic fitting or a pulse shape fitting (detect signals forms). However our signals differ in shape in a high range and the small intensity signals are affected by the white random noise hence, a parabolic fitting is not suitable. Sometimes the easiest way is the more optimal. Indeed, a search for the highest point in the window has done a good performance. On the other hand, due to the absence of pulse shape fitting, area values have been obtained by simply integration. Area values will be highly affected by noise has we will see in V.

IV. ENERGY CALIBRATION OF THE PULSE AMPLITUDE SPECTRA

A typical pulse-height spectrum from a ^3He proportional counter is shown in figure 2. The shape in the spectrum is a manifestation of the proton and tritium trajectory after the nuclear interaction.

The characteristic feature of ^3He spectra is the presence of a full-energy peak that act for the collection of the energy deposited by the proton and tritium. Therefore, the full-energy peak represents the 764 keV released in the interaction with the neutron. A proton edge can be seen at the left of the full-energy peak (574 keV) and a wide peak of 191 keV for the tritium. After the tritium edge, one can see a wide valley corresponding to noise and piled-up gamma-ray events that do not correlate with the nuclear reaction [2].

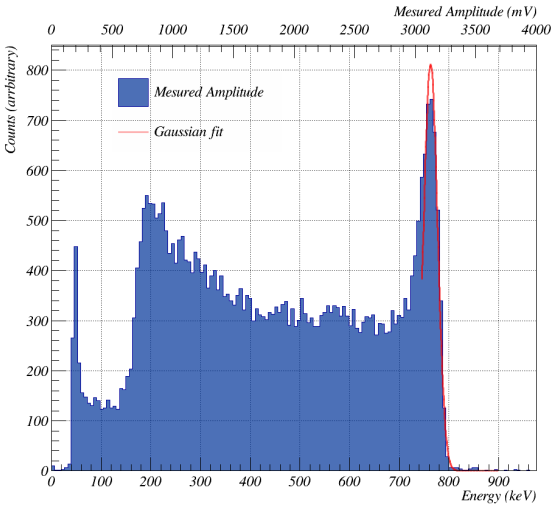

FIG. 2: Calibrated spectra of V61 for the amplitude. At the upper x-axis mesured amplitude is shown. At the bottom x-axis the calibrated values apying the equation REF EQ. In red the gaussian fit with in the selected range.

A. Trigger Threshold

Trigger threshold is critical, a too low threshold could detect noise as a pulse. Although with a low threshold, amplitude spectra will maintain the same shape, it also decreases resolution and introduce wrong area integrations inside the area spectra collection-range and increases linearly computation time. Furthermore, a to high threshold simply will only detect events of high energy and leave behind true events.
In order to obtain the best spectra, first, we have selected a minimum threshold for each detector. Manually we have found the smallest signal in the movie and performed a study, selecting the best threshold value to get rid of noise and pile-up gamma rays without affecting the collection-range. An optimal trigger threshold should fall in the valley between the gamma-rays and the tritium edge.

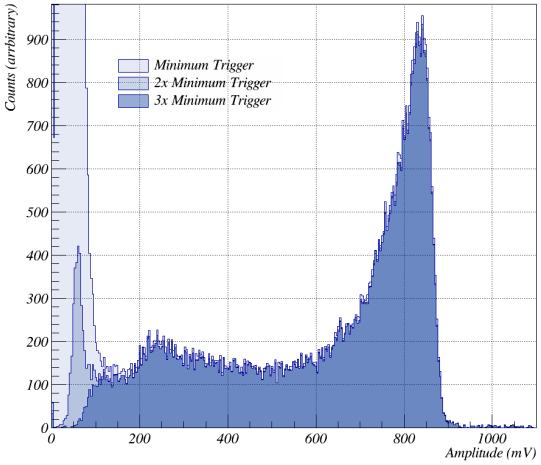

FIG. 3: Spectra for the LND detector choosing three different values for the trigger. With the minimum trigger, it is clear to see the inclusion of noise data points.

B. Calibration

Once we have the right trigger, we can apply a linear calibration knowing that the full-energy peak is at 764 keV. The first step is to rebin the histogram until we have a significant shape of the spectra. Furthermore, a gaussian shaped fit is applied within a selected range and accurate until the best fit is obtained. Finally, the gaussian parameters are extracted and the equation is solved.

$$E = Ax \tag{4}$$

Where E is the energy, 764 keV, x is the mean of the gaussian fit and A the calibration constant searched. A calibration based on amplitude is shown at figure 2. A calibration constant for the amplitude and the area is obtained for every detector and voltage operation. The values are shown in results V.

V. RESULTS

We present here the results of the developed digital pulse analysis. As shown in upper sections we have a success in the identification of the pulses and the reconstruction of the ^3He spectra. Several histograms have been calibrated for each detector with different voltage operation. Aside from the means belonging to the gaussians fits, we also have extracted from the histograms the standard deviation of the full-energy peak, the FWHM, the mean of the histogram, the calibration constant and the resolution of the spectra. These parameters are shown in table I.

Paying attention to the resolution of the spectra is found that the higher operation voltage in the detector the better resolution in the spectra. That is in fact a consequence of the signal-to-noise ratio. Although in the amplitude spectra resolution only decreases by 2%, there is a real problem when integrating signals with a low signal-to-noise ratio. Resolution decreases by more than 10%. Lowering the operation voltage has a direct effect on the integration, that is because the rise and fall time are close to the background white noise frequency. Therefore, the noise at those runs has a bigger contribution to the total area. An example of the dispersion of amplitude values in front of the amplitude values is shown in figure 4

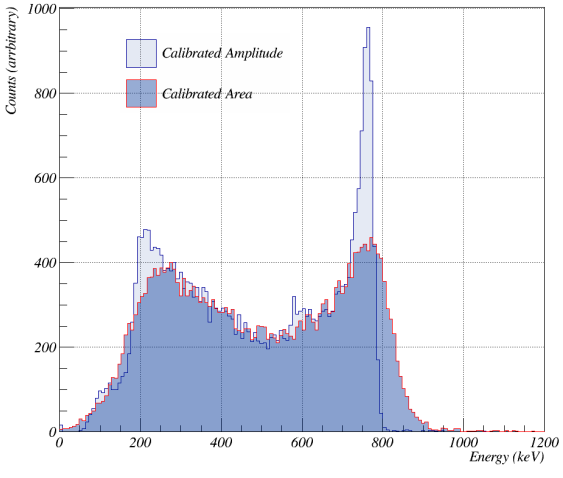

FIG. 4: Amplitude and Area spectra for the V60 detector and 880V of operational voltage. A high dispersion of area values is noticed.

Detector	Voltage (V)	Mean (mV)	± (mV)	Standard Deviation (mV)	± (mV)	FWHM (keV)	R (%)	Mean Amplitude (mV)	Calibration (10^6 e)
V61	1150	3512.390	6.422	67.020	3.632	22.623	1.908	2241.280	0.218
V60	1080	3142.500	4.361	53.314	2.855	20.077	1.697	1802.160	0.243
LND	1290	838.844	0.451	20.965	0.269	29.632	2.499	615.372	0.911
V61	930	502.336	0.598	11.228	0.349	26.501	2.235	392.516	1.521
V60	880	492.426	0.499	8.190	0.329	19.720	1.663	308.662	1.552
LND	1100	167.073	0.207	6.987	0.116	49.579	4.182	143.145	4.573
V61	930	500.679	0.423	11.982	0.273	28.374	2.393	385.023	1.526
LND	1100	164.464	0.192	6.665	0.102	48.050	4.053	136.819	4.645

TABLE I: Relevant information extracted from the amplitudes spectra.

Detector	Voltage (a.u)	Mean (a.u)	± (a.u)	Standard Deviation (a.u)	± (a.u)	FWHM (keV)	R (%)	Mean Area (a.u)	Calibration (a.u)
V61	1150	7.122E+07	1.965E+05	2.265E+06	9.555E+04	3.770E+01	3.180E+00	1.199E+02	1.073E-05
V60	1080	5.964E+07	9.653E+04	1.810E+06	5.666E+04	3.599E+01	3.036E+00	1.093E+02	1.281E-05
LND	1290	1.649E+07	2.253E+04	9.391E+05	1.329E+04	6.752E+01	5.695E+00	3.846E+02	4.633E-05
V61	930	9.219E+06	5.912E+04	1.312E+06	3.289E+04	1.688E+02	1.423E+01	2.402E+03	8.287E-05
V60	880	9.050E+06	2.014E-01	1.285E-02	2.648E-01	1.683E-06	1.420E-07	2.390E-13	8.442E-05
LND	1100	3.136E+06	2.204E+04	5.458E+05	1.055E+04	2.064E+02	1.740E+01	3.592E+03	2.436E-04
V61	930	9.156E+06	3.376E+04	1.354E+06	2.209E+04	1.753E+02	1.478E+01	2.591E+03	8.345E-05
LND	1100	3.033E+06	2.146E+04	5.511E+05	9.794E+03	2.154E+02	1.817E+01	3.914E+03	2.519E-04

TABLE II: Relevant information extracted from the areas spectra.

VI. CONCLUSIONS

- We have developed a viable digital pulse analysis and provided a good identification of events. Digital pulse analysis based on flash-ADCs has added flexibility to the signal processing methods. And not only that, but amplitude spectra also achieved a similar, and sometimes better, performance than analog ^3He proportional spectra given in the detector's datasheets.
- Clear linearity between amplitude and area values in max operating voltage values has been found, yet for lower operating voltages, noise background has affected our analysis causing the divergence of area values. Although the mean spectra area values are enough to use in a high-piled-up signal from a pulsed proton beam, a method based on the deconvolution of the signal [3] is thought to increase area resolution. A first approach to extract the parameters has been done. However, deconvolution methods are still waiting to be implemented.

Acknowledgments

I thank Ariel Tarifeño for offering all a tutor can be. I thank Michael Bacak for their help and work at the stage of data acquisition from n_TOF. I thank n_TOF collaboration for letting me the opportunity to see how investigation is done at CERN. I thank all of you who has supported my agonies and encouraged me though these years. To all, I owe you one.

[1] U. Abbondanno, G. Aerts, and F. Álvarez et all. The data acquisition system of the neutron time-of-flight facility n_tof at cern. *Nuclear Instruments and Methods in Physics Research Section A: Accelerators, Spectrometers, Detectors and Associated Equipment*, 538(1):692–702, 2005.

[2] T. W. Crane and Michael Paul Baker. Neutron detectors. 2020.

[3] Valentin T. Jordanov. Unfolding-synthesis technique for digital pulse processing. part 1: Unfolding. *Nuclear Instruments and Methods in Physics Research*, 805:63–71, 2016. Special Issue in memory of Glenn F. Knoll.

[4] C. Weiß et all. P. Žugec. Pulse processing routines for neutron time-of-flight data. *Nuclear Instruments and Methods in Physics Research Section A: Accelerators, Spectrometers, Detectors and Associated Equipment*, 812:134–144, 2016.

[5] Steven W. Smith. Chapter 15 - moving average filters. In *Digital Signal Processing*, pages 277–284. Newnes, Boston, 2003.

[6] C. Weiß, E. Chiaveri, S. Girod, and V. Vlachoudis et all. The new vertical neutron beam line at the cern n_tof facility design and outlook on the performance. *Nuclear Instruments and Methods in Physics Research Section A: Accelerators, Spectrometers, Detectors and Associated Equipment*, 799:90–98, 2015.